How does the atmospheric variability drive the aerosol residence time in the Arctic region?

M. Ménégoz, A. Voldoire, H. Teyssèdre, David Salas y Melia, Vincent-Henri Peuch, I. Gouttevin

Tellus SERIES B CHEMICAL AND PHYSICAL METEOROLOGY
PUBLISHED BY THE INTERNATIONAL METEOROLOGICAL INSTITUTE IN STOCKHOLM

How does the atmospheric variability drive the aerosol residence time in the Arctic region?

By M. MÉNÉGOZ[1]*, A. VOLDOIRE[2], H. TEYSSÈDRE[2], D. SALAS y MÉLIA[2], V.-H. PEUCH[2] AND I. GOUTTEVIN[1], [1]*LGGE, CLIPS, CNRS-INSU and UJF Grenoble, 54, rue Molière BP 96, F-38402, Saint-Martin d'Hères, Cedex, France;* [2]*Météo-France, CNRM-GAME, GMGEC/ASTER, 42 Avenue Gaspard Coriolis, 31057, Toulouse, France*

(Manuscript received 21 January 2011; in final form 19 October 2011)

ABSTRACT

This paper aims at characterising the impact of the atmospheric variability on the aerosol burden and residence time in the Arctic region. For this purpose, a global simulation using an emissions inventory from the year 2000 is performed for the period 2000–2005. The model thus describes a 6-yr evolution of sulphate, black carbon (BC) and mineral dust, whose variability is driven by the atmosphere only. Our simulation is validated, thanks to comparisons with surface observations. The aerosol residence time takes minimum values in fall: 4 d for sulphate and 8 d for BC and dust. It takes maximum values in June: 10 d for sulphate and 16 d for BC and dust. However, from one spring to another, it can vary by about 50% for sulphate, 40% for BC and 100% for dust, depending on the atmospheric variability. In June, sulphate, BC and dust burden averaged over the Arctic region reach respectively maximums of 1.9 mg[S] m^{-2}, 0.2 mg m^{-2} and 6 mg m^{-2}, characteristic of the so-called Arctic haze. From one year to another, these values can vary by 20% for sulphate, 10% for BC and 60% for dust.

Keywords: Aerosols, Arctic, atmosphere, residence time, pollutant transport

1. Introduction

The Arctic region was considered not polluted until the year 1950, when pilots flying over the Arctic observed strong pollution, reducing significantly the visibility (Greenaway, 1950). Then, different studies showed that the combination of strong emissions in the Northern hemisphere with the very specific Arctic meteorology could induce high concentrations of anthropogenic and natural aerosols in the Arctic atmosphere (e.g. Shaw, 1995; Stohl, 2006). The so-called Arctic haze provides a striking illustration of the intensity of this process in spring time. Sulphur compounds, black and organic carbon aerosols concentration in the Arctic atmosphere are notably affected by anthropogenic emissions from North America, South-eastern Asia and Europe. A significant part of carbon aerosols emitted during biomass-burning events in boreal and temperate regions is also transported towards the Arctic region (Lavoué et al., 2000). Moreover, transport of dust from African and Asiatic deserts towards the Arctic has also been observed (Pacyna and Ottar, 1986).

These aerosols alter local radiative fluxes, temperature profiles and cloud properties. Sulphate aerosols are known to strongly scatter solar radiation (Penner et al., 2001), inducing negative radiative forcing. On the opposite, strongly absorbing black carbon (BC) aerosols yield a positive radiative forcing (IPCC, 2007). Warming the atmosphere, BC aerosols can be responsible for enhanced cloud evaporation and hence a decrease in the fraction of solar radiation reflected by the cloud cover. This strong climatic retroaction is referred to as the 'semi-direct effect' of BC aerosols. BC aerosols also induce a strong positive radiative forcing when they are deposited on snow because they decrease the snow cover albedo (e.g. Jacobson, 2004; Flanner et al., 2007). Mineral dust is known to affect the atmospheric radiative balance by decreasing the solar radiation reaching the surface and scattering and absorbing the terrestrial radiation (Reddy et al., 2005). Overall, a better and quantitative knowledge of the atmospheric aerosol concentration is paramount to assess its radiative effects in the Arctic, a region particularly sensitive to climate change (IPCC, 2007). Recent studies have

*Corresponding author. email: menegozmartin@yahoo.fr

Citation: Tellus B 2012, **64**, 11596, DOI: 10.3402/tellusb.v64i0.11596

evaluated the aerosol transport into the Arctic, based on transport model simulations (Stohl, 2006; Bourgeois and Bey, 2011) or on multimodel chemical-transport model analysis (Shindell et al., 2008). According to Shindell et al. (2008), sulphate and BC Arctic surface concentrations are mostly affected by European emissions, whereas their 250 hPa concentrations mainly originate from North American and Asian emissions. Gong et al. (2010) observed a decrease in sulphate and BC concentrations during the last 30 yr at Alert, North America and suggested that this trend corresponds to a decrease in Eurasian emissions, which results in an increase in the relative influence of American emissions on the Arctic aerosol concentration. Sharma et al. (2006) and Hirdman et al. (2010) also observed a decrease in the aerosol concentration at different Arctic sites. Based on retro-trajectory analyses, they explain this decrease by a reduction of emissions in the Northern hemisphere. According to Hirdman et al. (2010), the long-term trend of the atmospheric variability can explain only a minor fraction of the overall downward trend seen in the Arctic BC measurements. However, Sharma et al. (2006) pointed out that pollutants surface concentrations at some Arctic stations can be quite different from one year to another due to atmospheric inter-annual variability: pollutants surface concentrations in Northern America are 40% higher over the years 1991–1994 than over the years 1995–1998, a difference they explained by a more frequent positive phase of the North Atlantic Oscillation in the first period than in the second, which brings more pollutants from Eurasia into the Arctic via a stronger Siberian anticyclone.

Our study is based on a multiyear aerosol simulation using constant emissions to evaluate the impact of the atmospheric inter-annual variability on the aerosol burden in the whole Arctic atmosphere. We computed a global simulation from 2000 to 2005, but for the purpose of this study, we consider a domain centred over the Arctic region, between 60 °N and 90° N. In particular, we focus on the detailed balance of three aerosol species: sulphate, BC and mineral dust.

The chemical transport global model used in this study is described in Section 2, along with a sensitivity experiment to in-cloud scavenging. In Section 3, comparisons with surface observations enable to validate the model in the Arctic region and to discuss both seasonal and inter-annual variations of the surface atmospheric concentration of aerosols. Section 4 details the balance between sinks and sources of aerosols in the Arctic atmosphere. This analysis helps explaining the intra- and inter-annual variability of both the residence time and the aerosol burden in the Arctic region. A comparison of the Arctic atmospheric aerosol burden in spring 2001 and spring 2004 is exposed in Section 5, before final conclusions in Section 6.

2. Experimental configuration

2.1. The MOCAGE Chemistry-Transport Model (CTM)

For this study, a 6-yr global simulation was performed with the MOCAGE model (Teyssèdre et al., 2007). MOCAGE is used with a T42 Gaussian grid (about 2.8° × 2.8° horizontal resolution) and with 47 layers from the surface to 5 hPa. Seven levels are within the planetary boundary layer (PBL), 20 in the free troposphere and 20 in the stratosphere. The vertical coordinate is hybrid (sigma, P). The first layer is 40 m thick, whereas the resolution above 300 hPa is constant with altitude, around 800 m. In our simulation, the air temperature, humidity, pressure and wind components used to drive MOCAGE consist of the 6-hourly analyses of the European Centre for Medium-Range Weather Forecasts (ECMWF) IFS model. A semi-lagrangian scheme is used for the advection of tracers and chemical compounds. It is based on the work of Williamson and Rasch (1989) and is not supposed to conserve mass as soon as the grid is irregular. A simple correction scheme is, therefore, applied to ensure total mass conservation during transport. Further details on the transport in MOCAGE are presented in Josse et al. (2004), who validated the transport in MOCAGE comparing modelled and observed radon fields. Time steps are 1 h for advection and 15 min for subgrid scale processes. Turbulent diffusion follows Louis (1979), whereas the convection scheme (mass-flux type) relies on Bechtold et al. (2001). The representation of dry deposition, based on the work of Wesely (1989), is detailed in Michou and Peuch (2002). In-cloud and below-cloud scavenging representation for gases is based on Mari et al. (2000).

2.2. Aerosols in the MOCAGE CTM

MOCAGE can simulate the evolution of three types of aerosols compartmented in size-related bins: dust aerosols are divided into five bins between 0.01 μm and 100 μm; and BC and sulphates are both divided into four bins between 0.001 μm and 10 μm. Organic and nitrate aerosols, as sea salt, have not yet been implemented in our model and are therefore not taken into account in this study. The model configuration used here is quite similar to the one used in Ménégoz et al. (2009): emissions of both primary aerosols and aerosol precursor gases of the 'AEROsol Comparisons between Observations and Models' (AEROCOM) global inventory are used. Dentener et al. (2006) presented a complete description of this inventory, which is representative of the year 2000. We used the AEROCOM emissions representative of year 2000 to drive the 6 yr of our 2000–2005 simulation, to evaluate how the atmospheric

variability affects the aerosol burden and residence time. This protocol allows to exclude the aerosol burden variations induced by the inter-annual variability of real emissions. Emissions of BC, SO_2, H_2S and SO_4^{2-} are constant over the year in the AEROCOM inventory, except for biomass-burning emissions that display monthly variations. Although daily variations of DMS and dust are accounted for in the AEROCOM inventory, we used the monthly averages of these fields for our 6-yr simulation because we assumed that daily variations of these emissions are very different from one year to the other, and that the daily variations of 2000 would not be relevant for the whole 2000–2005 period. The anthropogenic elementary sulphur of 2.5% is supposed to be directly emitted as SO_4^{2-} (Dentener et al., 2006), the rest originating from SO_2. To avoid too strong vertical gradients within the PBL, emissions are distributed over the five lowest levels of the model that cover an average height of 600 m. The chemical formation of sulphate is modelled as described in Pham et al. (1995), based on a simple sulphur chemical scheme and climatologies of oxidant species. This model is described in Ménégoz et al. (2009). The climatologies of oxidants originate from a previous MOCAGE 6-yr simulation using a detailed scheme for the chemistry of oxidants in the atmosphere (see Teyssèdre et al., 2007).

2.3. *Physics of aerosols in the model*

Aerosols are removed from the atmosphere by three main sinks: dry deposition due to the contact of the atmospheric flow with the earth surface; sedimentation implied by gravitational forces; and wet deposition due to the presence of water droplets in the atmosphere (Seinfeld and Pandis, 2006). The parameterisations of dry deposition and sedimentation in MOCAGE are based on Seinfeld and Pandis (2006) and are presented, respectively, in Nho-Kim et al. (2004) and Martet et al. (2009). As explained in Section 2.2, some aerosol species, in particular sea salt, organics and nitrate aerosols, are not taken into account in our model. We defined aerosol size classes following the recommendations of the AEROCOM project: those classes are characteristic of real aerosols including different chemical species—both internally and externally mixed. In our model, these aerosol size classes are applied to sulphate, BC and dust. Even with missing species, we assume that it was the best protocol to describe realistically sedimentation, dry and wet deposition that are very dependent on the aerosol size.

MOCAGE describes both below-cloud and in-cloud scavenging. Below-cloud scavenging is aerosol adsorption by falling raindrops. Its parameterisation is based on Seinfeld and Pandis (2006). In-cloud scavenging designates both the droplet activation by aerosols and the adsorption of particles by airborne cloud droplets. This process is a major sink for aerosols, especially for soluble species (Boucher et al., 2002). Textor et al. (2006) pointed out that the differences of the in-cloud scavenging schemes used in global aerosol models explain the major part of the discrepancies between these models in terms of aerosol burden and residence time. In particular, the BC burden simulated in polar regions—far from the sources—can vary from orders of magnitudes according to the choice of the wet deposition scheme used in the model (Vignati et al., 2010). Here, we tried to improve the representation of in-cloud scavenging in our model. As Langner and Rodhe (1991), we compute a grid-cell dependent scavenging rate λ:

$$\lambda = \frac{\varepsilon \times \mathrm{R}}{\mathrm{L}}, \tag{1}$$

where R is the precipitation formation rate and L is the Cloud Liquid Water Content. ε characterises the transfer efficiency of aerosols towards droplets. It takes values between 0 and 1. We found very different values for this parameter in published model descriptions. As an example, Boucher et al. (2002) used a constant value equal to 0.7 for ε to simulate sulphate aerosol at the global scale. Stier et al. (2005) used seven classes of aerosols in their model. These ones are associated with different values of ε, varying between 0.10 and 0.99 depending on the aerosol size and solubility in their quite complex model. In our study, we considered that ε was proportional to L, as reported by various field campaigns (e.g. Kasper-Giebl et al., 2000; Hitzenberg et al., 2001; Cozic et al., 2007):

$$\varepsilon = \alpha \times \mathrm{L} \tag{2}$$

For our study, we used the ε and L observations presented in Kasper-Giebl et al. (2000) to calibrate α both for sulphate and BC aerosols. As dust scavenging ratio is quite unknown, we considered in a first assumption that $\alpha = 1$ for this aerosol.

In the real world, these parameters are not necessarily constant over the lifetime of an aerosol, from the emission to its deposition. Through ageing processes, particles generally become more hydrophilic and are scavenged more efficiently. This is particularly true for BC aerosols that are relatively hydrophobic when freshly emitted and that become quite hydrophilic after several days in the atmosphere as they are covered by soluble species such as sulphate, nitrate and sea salt (Riemer et al., 2004). The observations of Kasper-Giebl et al. (2000) we used to infer our parameters values originate from mountainous areas, where aerosols are relatively aged and are therefore relatively soluble in comparison with recently emitted atmospheric aerosols. For this reason, our model probably overestimates aerosol solubility on average. However, many other different processes drive the solubility and

scavenging ratio of aerosols. The phase of water droplets, the aerosol size and the aerosol concentration itself can strongly impact these parameters (Henning et al., 2004; Cozic et al., 2007) with an order of magnitude exceeding the temporal variations considered in some models. All these aspects could be improved by future developments.

For each aerosol, ε has an upper bound, as described in the following. A similar in-cloud scavenging parameterisation was used in Ménégoz et al. (2009) to simulate sulphate aerosol over Europe, which resulted in an overestimated sulphate atmospheric concentration when compared with surface observations. As Kasper-Giebl et al. (2000) never observed ε values lower than 0.2 for sulphate, we made here a sensitivity experiment setting an ε lower bound equal to 0.2 for this aerosol. In addition, only scavenging by liquid droplets was considered in Ménégoz et al. (2009). Ice droplets scavenging was neglected that could also explain a part of the overestimation of the modelled sulphate concentration. Over the Arctic region (from 60 °N to 90 °N), snow falls are far from being negligible in comparison to liquid precipitation in the meteorological analyses used for our simulation (Fig. 1). As a consequence, scavenging by ice droplets should not be neglected. Therefore, we performed another sensitivity experiment considering both scavenging by liquid and solid droplets. As a first assumption, we considered that the transfer efficiency of aerosols towards droplets (ε) does not vary according to the phase of the droplet. Eqs. (3) to (5) describe the values of ε that we adjusted on the observation of Kasper-Giebl et al. (2000):

$$\varepsilon_{\text{sulphate}} = \max(0.2; 3L) \quad \text{for } L \le 0.3; \qquad \varepsilon_{\text{sulphate}} = 0.9 \quad \text{for } L > 0.3 \tag{3}$$

$$\varepsilon_{BC} = 1.2L \quad \text{for } L \le 0.6; \ \varepsilon_{BC} = 0.6 \quad \text{for } L > 0.6 \tag{4}$$

$$\varepsilon_{\text{dust}} = L \quad \text{for } L \le 0.6; \ \varepsilon_{\text{dust}} = 0.6 \quad \text{for } L > 0.6 \tag{5}$$

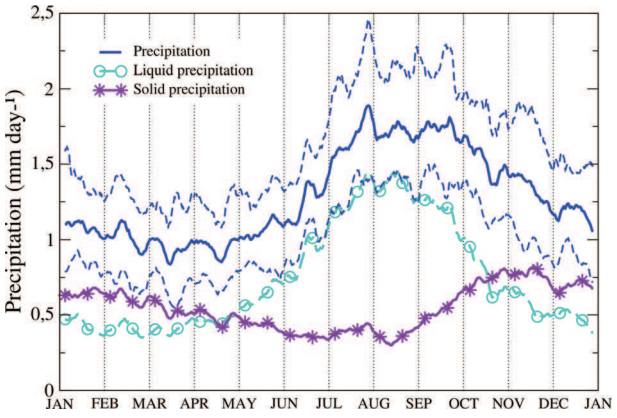

Fig. 1. Liquid, solid and total precipitation in the Arctic region (60 °N to 90 °N) from the operational ECMWF analyses. Dashed lines represent the extreme values reached during the 6-yr simulation.

L is the total cloud water content (both ice and liquid droplets).

Table 1 shows the global burden and the residence time for aerosols without (param_old) and with (param_new) ice droplets scavenging. The new lower bound for $\varepsilon_{\text{sulphate}}$ (0.2) is taken into account in param_new. Furthermore, Table 1 shows the mean and the range of the 16 global chemistry transport models involved in the AEROCOM inter-comparison exercise (Textor et al., 2006). In the 'param_old' column, the values in parenthesis correspond to the values simulated without ice droplets scavenging, but with the new lower bound for $\varepsilon_{\text{sulphate}}$. Putting this 0.2 lower bound for ε decreases significantly—about 25%—both the burden and the residence time of sulphate. Moreover, considering ice droplets scavenging decreases by 30%–40% the burden and the residence time of sulphate, BC and dust in our global simulation. As we can see in Table 1, both the burden and the residence time of sulphate and BC simulated with the old parameterisation seem to be over estimated, as they have very high values in comparison with the other models. The new parameterisation hence helps simulating sulphate and BC burden and residence time within the range of the AEROCOM models. The impact of the new parameterisation on dust modelling can barely be assessed because both old and new parameterisations lead to dust burden and residence time in the lower part of the range of the AEROCOM simulations. The low value of the modelled dust burden in comparison with the other AEROCOM simulations is clearly explained by the low atmospheric residence time of this aerosol in our model. This is mainly due to the representation of dry deposition, which is more efficient in our model than in the other AEROCOM models. Dry deposition is the main sink for dust. This flux is quite difficult to estimate and differs widely from one model to another (Textor et al., 2006).

Evaluating the mean residence time of aerosols at the global scale is difficult as it varies a lot over the Earth surface, depending on air humidity and aerosol size and physical properties that drive the scavenging ratio. From a few days for common species (3.3 d for sulphate as an example according to Seinfeld and Pandis, 2006), it can reach higher values when far from the sources or in dry atmosphere. Stohl (2006) for instance reported an aerosol residence time up to 20 d in the Arctic atmosphere. These aspects are discussed in detail in Section 4.

With its improved parameterisation, our model thus simulates burdens and residence times for sulphate, BC and dust within the range of AEROCOM models. As scavenging by ice droplets is taken into account in our model, aerosol burden and residence time are expected to be well simulated in the Arctic region, where snow represents a large part of the precipitation (Fig. 1). A further evaluation

Table 1. Global burden (Tg[S] for sulphate, Tg for BC and dust) and residence time (days) of sulphate, BC and mineral dust, as simulated over the year 2000 by MOCAGE with the old and the new parameterisations of scavenging (columns Param_old and Param_new) and results from the AEROCOM intercomparison exercise (Textor et al., 2006; mean values of the 16 global chemical transport models in the column Aerocom mean, with range of values in square brackets)

	Burden			Residence time		
Aerosol	Param_old	Param_new	Aerocom mean	Param_old	Param_new	Aerocom mean
Sulphate	1.15 (0.85)	0.60	0.7 [0.3–1.2]	9.5 (7)	5.0	4.12 [2.9–5.4]
BC	0.20	0.14	0.2 [0.11–0.37]	9.4	6.6	7.12 [5.2–10]
Dust	13.20	9.60	21.3 [6–30]	2.9	2.1	4.14 [1.2–7]

Note: Contrary to the old parameterisation, the new one includes scavenging by ice droplets and a 0.2 lower boundary for sulphate transfer coefficient ε. Values in brackets in the Param_old columns refer to a simulation without ice droplets scavenging but using a lower 0.2 boundary for ε sulphate.

of our model is performed in Section 3 with a comparison of model outputs with observations.

3. Modelled and observed Arctic aerosol surface concentration

As shown in many previous studies (e.g. Stohl, 2006; Shindell et al., 2008), the anthropogenic activities in Europe are the first responsible for the Arctic aerosol pollution. In the following, our simulation outputs are thus compared with aerosol measurements carried out within the European Monitoring and Evaluating Program (EMEP, Hjellbrekke, 2004). This network provides aerosol measurements at high latitudes, which constitute the relevant area for our study. We also show in the following comparisons between the sulphate concentration modelled and observed at three high-latitude northern American sites: Denali National Park and Barrow (Alaska) and Alert (Canada). Note that we analyse here only the non-sea salt sulphate aerosol. All the sulphate associated with sea salt in the observations were removed from the data based on a sulphate to sodium seawater ratio (Quinn, person. com. and Quinn et al., 2000). The ability of MOCAGE to simulate dust transport and deposition events was validated by Martet et al. (2009) on the basis of comparisons with satellite observations. However, due to the scarcity of available long-term observations for mineral dust, we show in the following comparisons between model and observations only for sulphate and BC.

3.1. The sulphate atmospheric concentration

Figure 2 shows the atmospheric sulphate surface concentration modelled with MOCAGE and observed at EMEP stations located north of 60 °N. Overall, model and observations yield atmospheric concentrations of similar orders of magnitude at the different EMEP sites. However, MOCAGE underestimates (station NO_3, Spitsbergen, 11.8 °E, 78.9 °N) and overestimates (station IS1, Island, 338 °E, 64 °N; station FI1, Finland, 27 °E, 60 °N) slightly the values observed at some stations.

The sulphate surface concentration can vary by a factor 5 between the different EMEP stations, depending on the proximity of the anthropogenic sources. Based on EMEP averaged observations (Fig. 2, down right), the sulphate concentration is higher in Eastern than in Western Europe, due to the proximity of the anthropogenic sources and to the general atmospheric circulation characterised by westerly winds. For these reasons, the sulphate monthly mean concentration takes values between 0.2 and 2.5 μg[S] m^{-3} in Russia and Northern Finland (stations RU1, FI1 and FI2), whereas it does not exceed 0.6 μg m^{-3} near the western coast of Norway and in Island (stations NO_2 and IS1). As explained in the next section and in numerous previous studies (e.g. Shindell et al., 2008; Hirdman et al., 2010), the aerosol concentration in the Arctic region is strongly influenced by continental anthropogenic emissions. The sulphate concentration observed at the Spitsbergen station (NO_3, 11.8 °E, 78.9 °N) is, therefore, expected to be affected by anthropogenic sources; it varies between 0.05 and 0.5 μg[S] m^{-3}.

At the EMEP sites considered here, all the observations show a strong seasonal cycle, with a minimum occurring in fall or at the end of summer, and a maximum occurring in winter or in the early spring. The sulphate concentration can vary by a factor 10 over 1 yr. Our model simulates quite well the seasonal cycle amplitude as well as its phase, except in the Spitsbergen station (station NO_3) where the simulated maximum occurs from one to three months after the observed maximum.

Figure 3 shows the sulphate concentration modelled and observed at three stations in North America. At these remote high latitude locations (63.7 °N, 71.3 °N and 82.39 °N), the atmosphere is less polluted than in the EMEP stations, and the monthly mean sulphate concentration never exceeds 0.5 μg[S] m^{-3}. The observed values

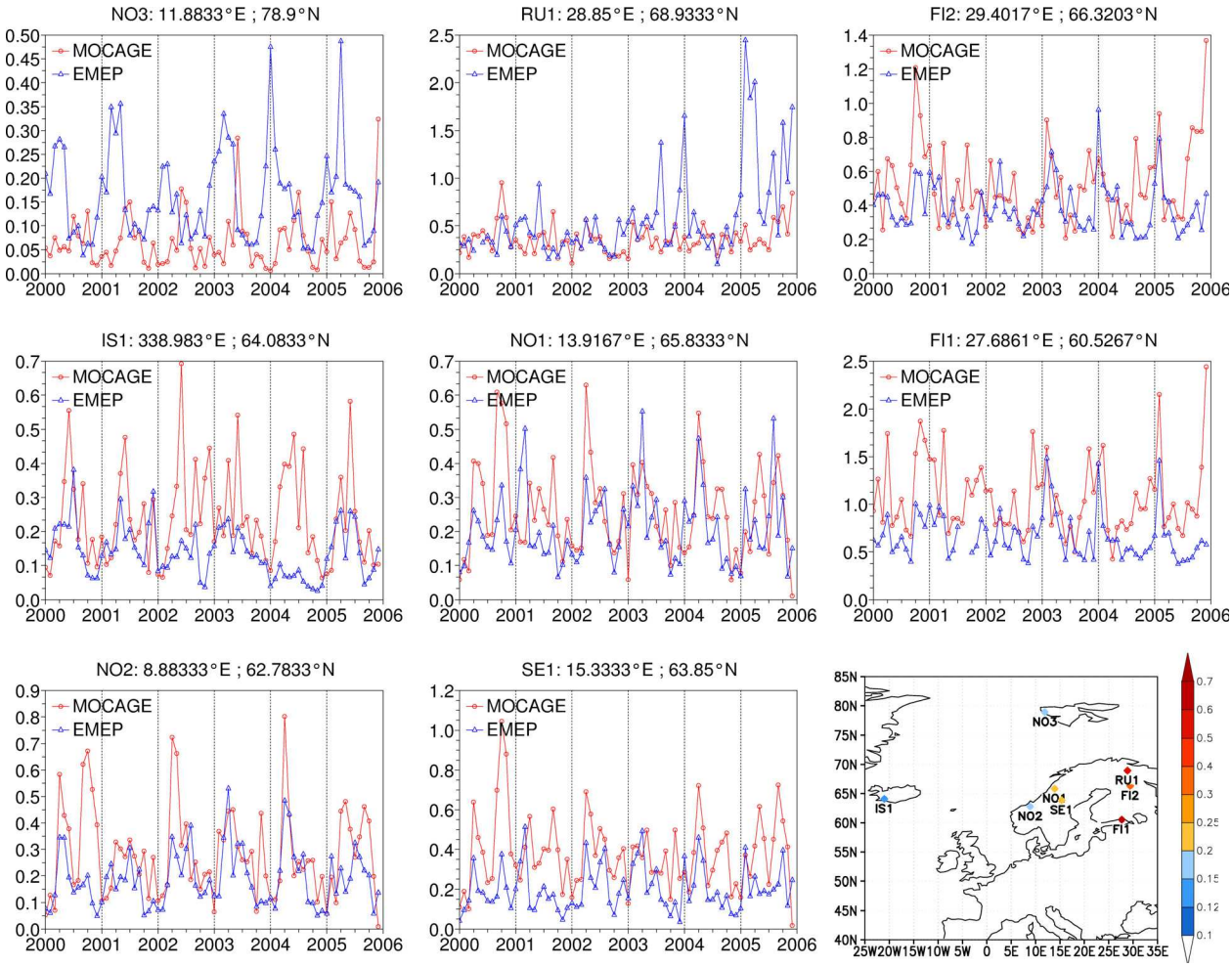

Fig. 2. Monthly mean of the atmospheric sulphate surface concentration (μg[S] m^{-3}) simulated by MOCAGE (red) and observed at EMEP stations (blue). Bottom right: the map displays the location of the stations and the 2000–2005 averaged observed sulphate concentrations.

show also a strong seasonal cycle, with a maximum occurring in winter or in early spring and a minimum occurring in fall. In contrast with the European domain, the concordance between model and observations is quite poor at these North American stations: the model underestimates the sulphate concentration by a factor 1–5, and the modelled maximum values are reached one or two months later than in the observations.

The discrepancies between our simulation and the observations may be partly explained by uncertainties in the emission inventory. The AEROCOM inventory is based on many different global or regional emissions studies (Dentener et al., 2006) that may contain some biases. As an example, Prank et al. (2010) recently showed that SO_2 emissions in the Kola peninsular are strongly underestimated in all emission inventories. These sources being located at relatively high latitude, they clearly affect the aerosol load in the Arctic.

We have to keep in mind that the AEROCOM emission inventory used in our simulation provides constant anthropogenic sulphur emissions over the year. Most studies dedicated to global inventories estimate that there is insufficient information to provide seasonal variations for anthropogenic sulphur emissions (e.g. AEROCOM described in Dentener et al., 2006; CMIP5 emissions described in Lamarque et al., 2010). The end user is free to describe a temporal variation of the sulphur emissions in the global aerosol simulations. Meij et al. (2006) modelled the sulphate surface concentration over Europe with two different emissions inventories. In their study, the sulphate concentration is underestimated in winter and overestimated in summer when using the constant emissions of the AEROCOM inventory. With the EMEP emission inventory, which entails higher emissions in winter and lower emissions in summer, they obtained a better agreement with the observations. In our study, the amplitude of the

sulphate concentration annual cycle modelled in Europe at the surface is, therefore, probably underestimated. However, we did not want to include seasonal variations in our global simulation, as the seasonal variations of emissions over all the industrialised areas of the globe are difficult to evaluate. Moreover, emissions uncertainties are known to be of a second order in the accuracy of the aerosol models in comparison with their ability to describe transport, aerosol removal and chemical processes both for regional studies (Meij et al., 2006) and for global studies (Textor et al., 2007). In their study, Meij et al. (2006) showed that taking into account the seasonality of the sulphur emissions in Europe could modify by 20% the sulphate concentration modelled at the surface. Such variations are largely smaller than the variability modelled in our 6-yr simulation.

As our model describes quite well the sulphate concentration in polluted regions (see the southernmost stations of the EMEP domain in Fig. 3.1), we estimate that the bias in the emission inventory is not responsible for the strong bias in our simulation (Fig. 3). The model bias probably originates from the description of transport and removal processes. Bourgeois and Bey (2011) found that their CTM describes quite correctly the transport of chemical species towards the Arctic. However, they identified wet deposition parameterisation as the major source of incertitude in their CTM. The agreement between observations and simulations was improved by including an optimised representation for this sink in their model. As described in Section 2.3, our globally modelled aerosol burden is very sensitive to the scavenging coefficient. We tried to adjust this coefficient, which partly corrected our simulation biases. However, this coefficient is far from being constant, as it depends both on particles properties and clouds characteristics (Bourgeois and Bey, 2011). An improved description of wet deposition should clearly be the focus of future developing work. Nevertheless, we assume that even with some biases, we can use our model to analyse the inter-annual variability of the aerosol load in the Arctic.

Except for the oceanic emissions, which exhibit monthly variations and are largely weaker than anthropogenic emissions near the EMEP stations (not shown), our simulation is then based on constant sulphur emissions. The modelled variability in sulphate surface concentration is, therefore, essentially driven by atmospheric variability in our simulation. The modelled and the observed sulphate concentration inter-annual variabilities being quite similar, we can assume that the real emissions variability play a minor role in the variability of the sulphate concentration at the EMEP sites from 2000 to 2005. Moreover, no clear trend is detectable in the observed concentrations over the 6 yr, indicating few evolutions in the anthropogenic emissions from 2000 to 2005.

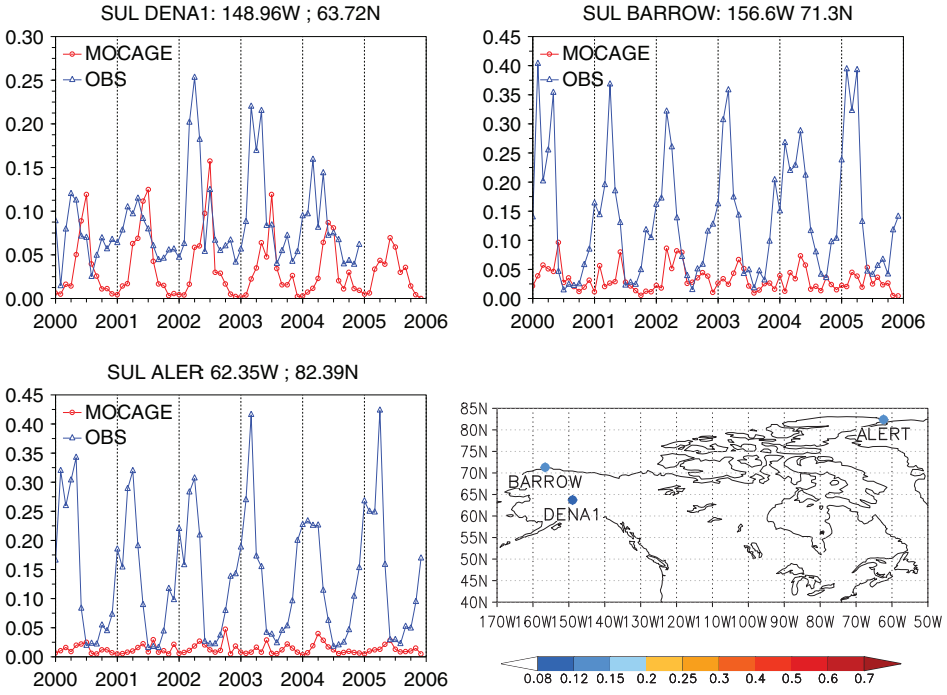

Fig. 3. Monthly mean of the atmospheric sulphate surface concentration (μg[S] m^{-3}) simulated by MOCAGE (red) and observed at Denali national Park, Barrow and Alert (blue). Bottom right: the map displays the location of the stations and the 2000–2005 averaged observed BC concentrations.

3.2. The BC atmospheric concentration

Figure 4 shows the atmospheric BC concentrations modelled with MOCAGE and observed at some EMEP stations. Measuring the atmospheric concentration of BC is more complicated and more uncertain than measuring sulphate concentrations (e.g. Hjellbrekke, 2004; Sharma et al., 2004). For this reason, few atmospheric BC measurements are currently available. As a consequence, only three EMEP sites are considered in this study, and two of them are unfortunately located south of 60 °N. Moreover, these measurements do not always cover the entire 2000–2005 period. We also show comparisons at two sites in North America in Fig. 5.

The BC concentrations display a wide range of magnitudes depending on the location of the observation site: about 1 $\mu g\,m^{-3}$ in high industrialised areas (station DE1, Fig. 4), 0.1 $\mu g\,m^{-3}$ in less polluted areas (station NO1, Fig. 4 and station DENA1, Fig. 5), and 0.01 $\mu g\,m^{-3}$ in Svalbard and in extreme Northern Canada, where the atmosphere is cleaner (station NO_2, Fig. 4 and station Alert, Fig. 5). Our model simulates quite well the order of magnitude of the BC concentration at the EMEP stations. However, it underestimates by a factor 1–5 the BC concentration at the southern EMEP site (station DE1), and by a factor 1–10 its value in the Svalbard station (NO_2). At NO1, the model is closer to the observed values. At the two northern American stations, there is a very strong discrepancy between our model and observations, by a factor 10 at Denali station and by a factor 50 at Alert (Fig. 5, note that the model values showed are $\times 10$). The discrepancies between modelled and observed values can originate both from model defaults or experimental uncertainties: Cavalli et al. (2010) pointed out that the BC atmospheric concentration can vary by a factor 5 depending on the observation protocol; on the model's part, both errors in emissions inventory and in deposition parameterisation can strongly affect the results of our simulation.

In our simulation, we used constant monthly biomass-burning emissions. This simplifying assumption certainly drives a large part our simulation biases. In the real world, biomass-burning emissions are quite variable, with substantial implications for the BC concentration observed throughout the atmosphere (Bourgeois and Bey, 2011). As explained in the following, other complex physical processes are coarsely represented in our model and may explain our model biases.

It is well known that, through ageing processes, BC is covered by soluble material and becomes therefore more hydrophilic (e.g. Conant et al., 2002). As explained in Section 2.3, the scavenging of our model is based on Kasper-Giebl et al.'s (2000) observations that have been

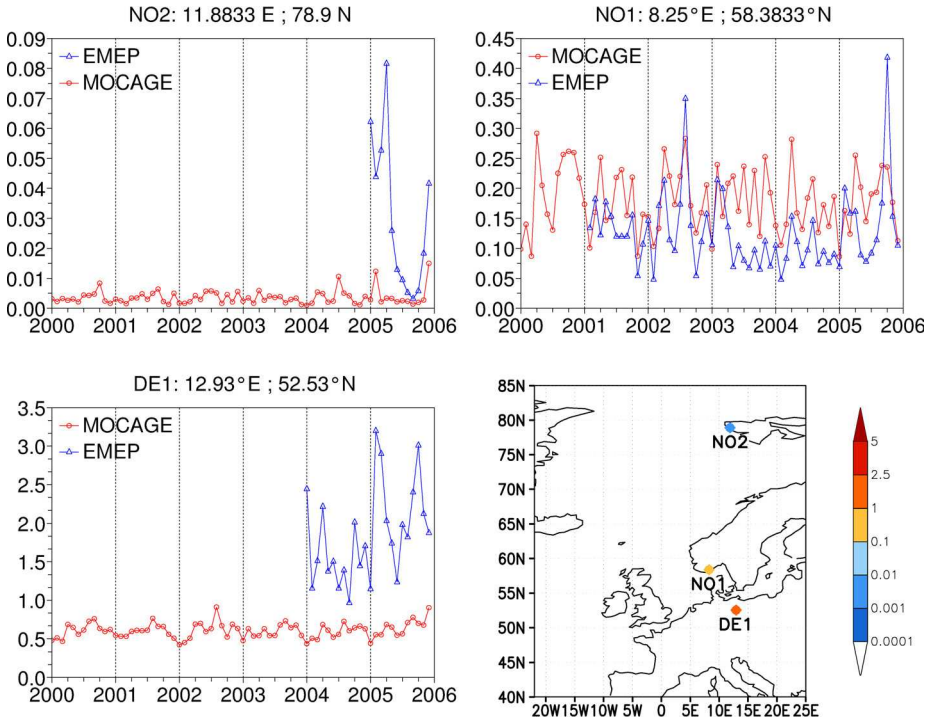

Fig. 4. Monthly mean of the atmospheric black carbon (BC) surface concentration ($\mu g\,m^{-3}$) simulated by MOCAGE (red) and observed at EMEP stations (blue). Bottom right, the map displays the location of the stations and the 2000–2005 averaged observed BC concentrations.

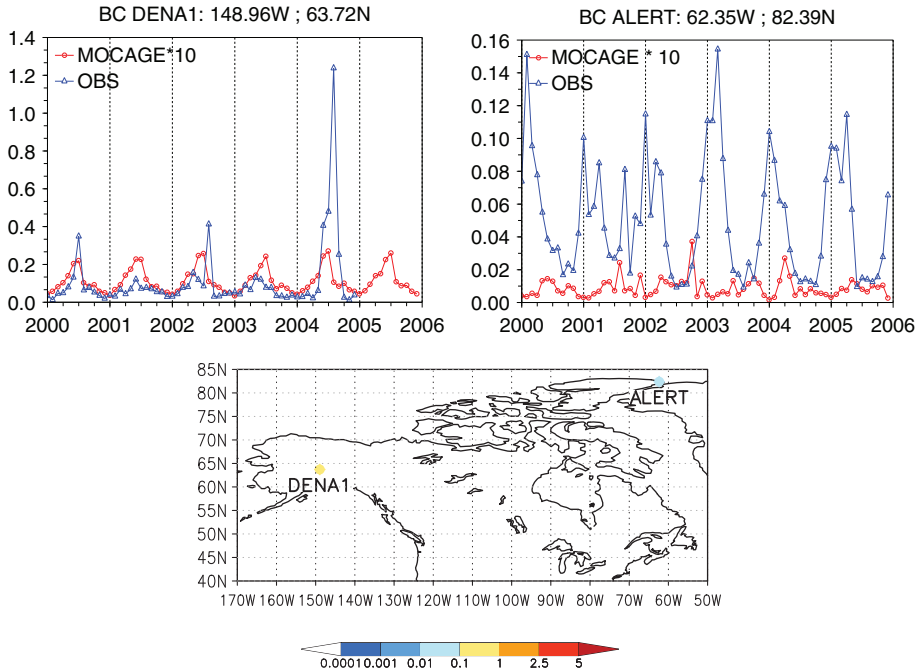

Fig. 5. Monthly mean of the atmospheric BC surface concentration ($\mu g\,m^{-3}$) simulated by MOCAGE (red) and observed at Denali national Park, Barrow and Alert (blue). Bottom right: the map displays the location of the stations and the 2000–2005 averaged observed BC concentrations.

carried out in a mountainous area, quite far from polluted areas. Therefore, we can assume that the scavenging coefficients used in this study are more appropriate for aged hydrophilic BC than for hydrophobic BC that exists close to particles' sources. This can provide an explanation for the general model underestimation of BC noticed in our study. Nevertheless, this assumption has to be taken very carefully seeing the complexity of the physical processes that have to be taken into account when modelling the atmospheric concentration of BC. As an example, we considered in our simulation the same scavenging ratio in all clouds. It can be a source of significant errors, as its value can be 10 times lower in mixed phase clouds in comparison to liquid clouds (Cozic et al., 2007).

Considering the difficulties of both simulating and measuring the BC atmospheric concentration, it is quite difficult to explain why the model and the observations are relatively concordant at the Norwegian EMEP site, whereas it is not the case at the other stations located in Northern Europe and in Northern America. Improving the representation of wet deposition in the model is likely to be the prior development to achieve more realistic BC simulation in the Arctic region. The global BC burden was shown to be very sensitive to wet deposition (Section 2). Bourgeois and Bey (2011) similarly pointed out the need of a correct evaluation of this process to estimate the part of anthropogenic BC transported to the Arctic region. Still, we assume that the BC atmospheric concentration intra- and inter-annual variabilities can be discussed on the basis of our simulations. The modelled variabilities display similarities with the observed variability. South of our domain, that is south of 60 °N, the BC atmospheric concentration does not have a marked seasonal cycle (see Fig. 4, stations NO1 and DE1). All the stations located north of 55 °N (NO_2, Fig. 4 and DENA1 and ALERT, Fig. 5) exhibit more pronounced seasonal cycles, both in our simulation and in the observations. At Alert and at the Spitsbergen station, maximum and minimum are, respectively, reached in winter and in summer. At the Spitsbergen station, the annual cycle modelled is in phase with that observed. It is not the case at the Alert station, where the annual cycle is very badly described by our model. We hope that the next developments planned for our model will lower these biases for future studies.

Still, on a general way, the seasonal variations of the BC atmospheric concentration can be explained by the seasonal variations of both precipitation—showing a maximum in summer (see Fig. 1)—and aerosol transport from polluted areas. The inter-annual variability of the BC concentration at these high latitude stations is clearly linked to the atmospheric variability. In particular, the monthly mean maximum does not occur at the same time each year and its amplitude can vary within 50% from one year to another. The context is quite different at the Denali

station (Fig. 5): Here, the annual cycle observed and modelled shows a maximum in summer and a minimum in winter. It is certainly due to local emissions associated with strong biomass-burning events occurring in summer in this region. This source is clearly visible in the emission inventory used for this study (not shown). At the Denali station, the inter-annual variability of the BC concentration is more pronounced in the observations than in our simulation due to the high variability of forest fires emissions, which is not considered in our simulation.

4. Intra- and inter-annual variations of the aerosols sinks and sources

4.1. Sulphate aerosol

Figure 6 shows the time evolution of the weekly mean burden, sinks and sources of sulphate integrated over the Arctic domain as well as the seasonal burden horizontal distribution and its zonal mean concentration by level over this domain. In the whole paper, each season is designated with the abbreviation of its months (DJF, MAM, JJA and SON). Over the 6 ys of our simulation, the averaged sulphate burden shows a strong seasonal cycle (Fig. 6, top left). It takes a minimum value close to $0.5\,\mathrm{mg[S]\,m^{-2}}$ in January and a maximum value close to $1.9\,\mathrm{mg[S]\,m^{-2}}$ in May. These extremums can vary by 20% from one year to another (Fig. 6, top left, dashed line). Such a cycle is explained by the seasonal variations of sinks and sources of sulphate over this region (Fig. 6, middle left). The main source of sulphate in the Arctic is the transport from southern polluted areas. The weekly mean value of this flux averaged over the six yr of our simulations ranges from 0.07 to $0.21\,\mathrm{mg[S]\,m^{-2}\,d^{-1}}$. Maximum values are reached in spring and fall, whereas minimum values are obtained in winter and summer. This 6-yr averaged annual cycle hides strong inter-annual variations (up to 100%), with overall minimum value of 0 and maximum value of $0.42\,\mathrm{mg[S]\,m^{-2}\,d^{-1}}$. The second source of sulphate over the Arctic region is the oxidation of SO_2. Its values are comprised all year long in a small range around $0.05\,\mathrm{mg[S]\,m^{-2}\,d^{-1}}$ except for spring values that are close to $0.1\,\mathrm{mg[S]\,m^{-2}\,d^{-1}}$. This maximum is explained both by the SO_2 transport from polluted areas, which is maximum in spring (not shown), and by DMS oceanic production that also reaches a peak value in June in high northern latitudes (not shown). In the Arctic atmosphere, one-third of the SO_2 is deposited on the surface, whereas the rest is quickly oxidised to sulphate via aqueous chemistry. Oxidation by gaseous chemistry is quasi equal to zero (not shown).

The main sink of sulphate over the Arctic region is wet deposition; dry deposition is quite negligible for this aerosol (Fig. 6, middle right). Wet deposition intensity depends both on precipitation and sulphate burden. For this reason, wet deposition seasonality correlates well with the seasonality of the transport of sulphate into the Arctic atmosphere. However, low precipitation in winter and early spring decreases wet deposition fluxes, while increased precipitation in summer and fall—with a maximum around July (Fig. 1)—limits the impact of sulphate transport towards the Arctic during these seasons.

The efficiency of aerosol sinks can be characterised by the aerosol residence time in the Arctic atmosphere (Fig. 6, bottom left). The aerosol residence time is computed here as the ratio between the aerosol burden and the sum of all the deposition fluxes. For sulphate, and on average over the 6 yr of our simulation, the residence time displays a marked seasonality with high values up to 11 d in June and low values around 4 d in November, December and January. These residences times can vary by 50% from one year to another (Fig. 6, bottom left, dashed lines). As our simulation was computed with constant emissions over the 6 yr, these variations are only related to the atmospheric variability.

In our simulation, we did not use tracers to trace back the geographical origin of the pollutants of the Arctic. However, we qualitatively discussed the likely contributions of Europe, North America and Asia to the pollution in the Arctic with regard to the modelled sulphate burden north of 60 °N (Figs. 6–8, top right). The Arctic region mostly affected by sulphate pollution is northern Eurasia, with three-month averaged burden values up to $3\,\mathrm{mg[S]\,m^{-2}}$ in spring. This pollution clearly results from the transport of sulphur compounds from European countries. Emissions from Eastern Asia have a moderate impact on the Arctic atmosphere, affecting a large region North of Siberia, with sulphate concentration reaching $1.5\,\mathrm{mg[S]\,m^{-2}}$ in spring. Northern American emissions seem to have a weaker impact on the sulphate concentration in the Arctic atmosphere. The three month averaged sulphate concentration around the North Pole varies between $0.25\,\mathrm{mg[S]\,m^{-2}}$ in winter and exceeds $1\,\mathrm{mg[S]\,m^{-2}}$ in spring. The lowest sulphate concentrations are found in central Greenland, where they never exceed $0.5\,\mathrm{mg[S]\,m^{-2}}$ due to the high altitude and strong winds of this region.

Sulphate transport from the northern hemisphere to the Arctic region is limited due to potential temperature difference between the Arctic region and polluted areas, forming the so-called Arctic front (e.g. Klonechi et al., 2003). However, Stohl (2006) showed that pollution from industrialised areas can penetrate into the Arctic atmosphere by two paths: within the atmosphere boundary layer if the potential temperature is the same between the emission region and the Arctic polluted region (path no. 1) or within the free troposphere if the potential

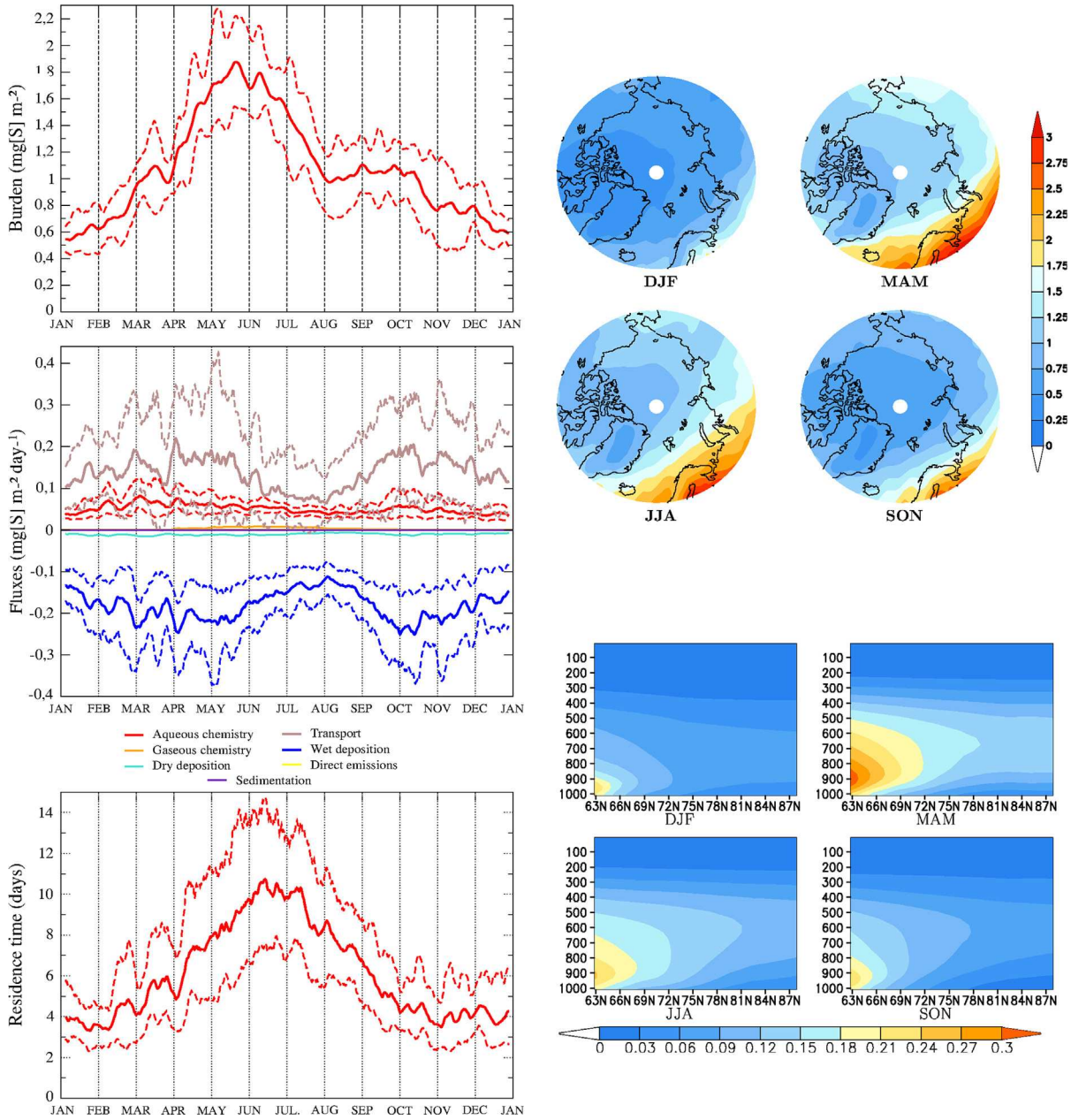

Fig. 6. Left: Burden, sinks, sources and residence time of sulphate averaged over the Arctic domain. The average is a weekly moving average of the annual cycle over 2000–2005; dashed lines represent the extreme values reached during the 6-yr simulation. Right, top: sulphate burden (mg[S] m^{-2}, 2000–2005 seasonal average); right, bottom: zonal mean of sulphate concentration (µg[S] m^{-3}, 2000–2005 seasonal average, pressure levels in hPa on the vertical axis). All graphs show MOCAGE model outputs.

temperature of the emission region is too high when compared with the Arctic region potential temperature (path no. 2). In DJF, only the emissions from northern Eurasia affect the Arctic atmosphere, occurring through the path no. 1, inducing maximum sulphate concentrations at relatively low altitude: maximum zonal means of 0.24 µg[S] m^{-3} and 0.06 µg[S] m^{-3} are respectively modelled at 950 hPa at 60 °N and 750 hPa at the North Pole in DJF (Fig. 6, bottom right). During the rest of the year, both paths no. 1 and no. 2 are efficient in our simulation, yielding maximum sulphate concentrations at higher altitudes: in MAM for instance, maximum zonal means of 0.3 and 0.15 µg[S] m^{-3} are, respectively, modelled at 900 hPa at 60 °N and 650 hPa at the North Pole. In this season, the low layers of the atmosphere are relatively weakly affected by pollution with a zonal mean of sulphate

concentration lower than $0.05\,\mu g[S]\,m^{-3}$ from 78 °N to 90 °N.

These characteristics of the aerosol transport from polluted areas to the Arctic region explain why the maximum sulphate concentration reported at the surface (EMEP data) occurs earlier—from one to three months—than the maximum value simulated over the whole Arctic atmosphere (Fig. 2 and Fig. 6, top left). Maximum sulphate concentrations at EMEP stations are generally observed at the end of the winter, whereas the maximum concentrations averaged over the whole thickness of the Arctic atmosphere occur later, in May. Such an evolution of the sulphate concentration profile throughout winter and spring is coherent with observations by Scheuer et al. (2003): in the frame of the aircraft campaign 'TOPSE', they observed an increase in the sulphate concentration in the low layers of the atmosphere throughout winter 2000. In spring, they reported a decrease in the sulphate concentration in the low layers of the atmosphere, whereas the sulphate concentration kept increasing in the higher layers (i.e. 2 km). Such an increase at high altitude may be due to the sulphate transport via the path no. 2. According to the analysis of Scheuer et al. (2003), the decrease in the sulphate concentration near the surface observed at the end of spring is reinforced by the increase of precipitation, enhancing scavenging processes.

4.2. *BC aerosols*

Figure 7 is the same as Fig. 6 but for BC. As for sulphate, the BC burden shows a well-marked seasonal cycle in the Arctic region (Fig. 7, top left). On average over the 6 yr, it has a minimum value of $0.06\,mg\,m^{-2}$ in January, and a maximum value of $0.23\,mg\,m^{-2}$ in July. These extremums can vary by 10% from one year to another (Fig. 7, top left, dashed lines). In spring and fall, the main source of BC in the Arctic is the transport from polluted areas. During these seasons, the 6-year average of this flux reaches values of $0.015\,mg\,m^{-2}\,d^{-1}$, whereas it is equal to zero in summer. As sulphate aerosol, BC transport displays strong inter-annual variations that can exceed 100%, with values varying between -0.015 and $0.4\,mg\,m^{-2}\,d^{-1}$ over the 6 yr of our simulation. This aerosol transport is responsible for the strong average burden in May (Fig. 7, top left). However, the maximum of BC burden occurring in July is explained by the emissions from boreal forest fires, which largely dominate over July and August (0.025 and $0.01\,mg\,m^{-2}\,d^{-1}$ according to the AEROCOM inventory). During these months, the BC transport budget is close to zero on average. It can be even negative, reaching a minimum of $-0.015\,mg\,m^{-2}\,d^{-1}$ (Fig. 7, left, dashed line) over our 6 yr of simulation. Wet deposition constitutes the main sinks for BC. As for sulphate, low precipitation levels associated with positive transport in spring induce a large increase in the BC burden. During fall, despite a significant transport from polluted areas, high precipitation increases wet deposition, inducing a decrease in the BC burden. Dry deposition is generally weak, except in summer when approximately one-third of BC is dry deposited. Due to high emission levels by forest fires, this dry deposition occurs close to the location of forest fires on the days displaying weak precipitation (not shown). The BC residence time has strong seasonal variations, with mean values of 8 d from October to January and mean values of 16 d in June (Fig. 7, bottom left). However, it has strong inter-annual variations (variations up to 40% from the 6-year mean value): its maximum and minimum are, respectively, 24 and 4 d over our 6-year simulation. Note that the shift in BC residence time at the beginning of July is induced by the biomass-burning emission that occurs suddenly during this month in our simulation. At that time, dry deposition becomes quite efficient in biomass-burning areas, which induces a quick decrease in the BC residence time in our simulation.

In spring and fall, BC burden patterns are quite similar to those of the sulphate burden (Fig. 7, top right), with values ranging from $0.075\,mg\,m^{-2}$ over Greenland to $0.3\,mg\,m^{-2}$ near polluted areas. During these months, the impact of European emissions seems to largely dominate the impact of Eastern Asian emissions. The influence of North American emissions is even weaker. In summer, the BC burden exceeds $0.3\,mg\,m^{-2}$ over large regions where forest fires take place. The rest of the Arctic is also more polluted, even above Greenland and the North Pole, where the BC burden reaches $0.15\,mg\,m^{-2}$. During all the winter, the BC burden is very low, never exceeding $0.05\,mg\,m^{-2}$, except over Alaska and Scandinavia, where it takes values up to $0.1\,mg\,m^{-2}$. At 60 °N, the zonal mean maximum of the BC concentration is reached close to the surface, around 950 hPa, ranging from $0.01\,\mu g\,m^{-3}$ in DJF to $0.1\,\mu g\,m^{-3}$ in JJA. At higher latitude, that is north of 70 °N, this maximum occurs at higher altitude, around 550 hPA, reaching values around $0.02\,\mu g\,m^{-3}$ (Fig. 7, bottom right). North of 75 °N, the BC concentration remains very low in the first thousand metres of the atmosphere all over the year, its zonal mean never exceeding $0.01\,\mu g\,m^{-3}$. This indicates a BC transport towards high latitudes following the path no. 2 presented in the last section. As for sulphate, BC maximum atmospheric surface concentration and maximum burden integrated over the whole atmosphere do not necessarily occur at the same period of the year. As an example, the maximum surface concentration modelled and observed in 2005 at the Spitsbergen (Fig. 4, station NO_2) occurs from December to April, whereas the maximum atmospheric BC burden simulated over this region rather occurs in spring

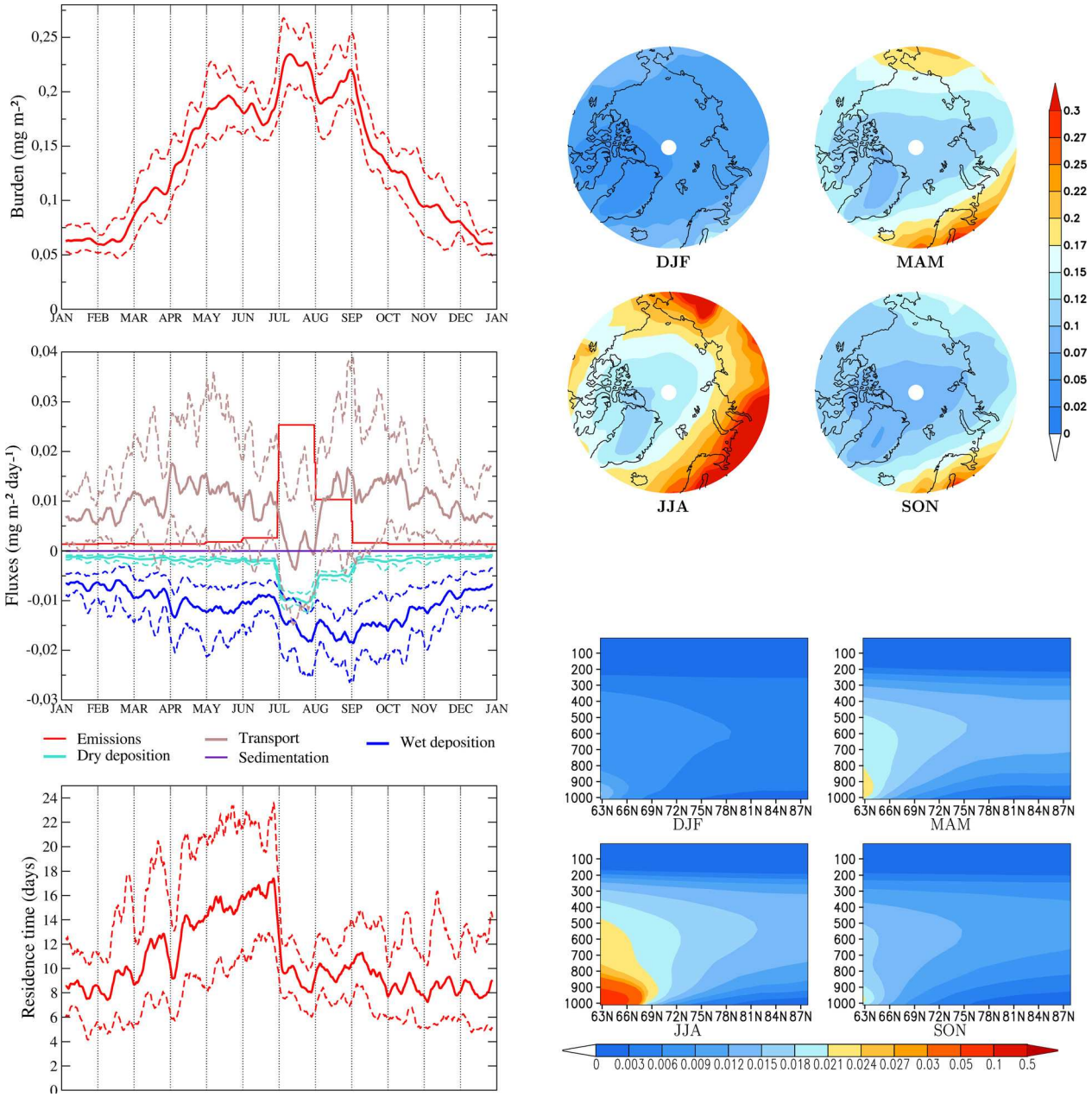

Fig. 7. Left: Burden, sinks, sources and residence time of BC averaged over the Arctic domain. The average is a weekly moving average of the annual cycle over 2000–2005. Dashed lines represent the extreme values reached during the 6-yr simulation. Right, top: BC burden (mg m^{-2}, 2000–2005 seasonal average); right, bottom: zonal mean of BC concentration (μg m^{-3}, 2000–2005 seasonal average, pressure levels in hPa on the vertical axis). All graphs show MOCAGE model outputs.

and summer for each of the 6 yr of our simulation (Fig. 7, top right, see the Spitsbergen region). Two factors may explain such a shift: first, the atmospheric BC surface concentration in Spitsbergen is particularly low in summer 2005 in comparison to simulation results for summers 2000–2004. This necessarily originates from particular atmospheric conditions, lowering the biomass-burning emissions influence in summer 2005. Second, as for sulphate aerosols, the transport of pollutants from Northern hemisphere to the Arctic region occurs mainly in the upper layers of the troposphere. The low layers are also affected by aerosol transport but to a lesser extent and earlier in the year.

Even under the assumption that our global aerosol model outputs can be used to analyse the main characteristics of BC transport towards the Arctic, the orders of

magnitude of the simulated BC concentrations have to be considered carefully. Modelling the atmospheric concentration of BC is quite challenging: Koch et al. (2009) compared different global aerosol model outputs with aircraft campaigns data. They found that models generally tend to strongly overestimate the aerosol atmospheric concentration between 0 °N and 50 °N in America. This is the contrary at latitude higher than 50 °N, where models underestimate it by a factor 1–10. According to Koch et al. (2009), such biases point out the need to improve the representation of scavenging and vertical dispersion processes in global aerosol models. Our model exhibits the same type of biases, and further developing work is required to improve the physical description of aerosol processes in the atmosphere. Further comparisons with aircraft data could then be realised in the future to validate the model ability at representing the BC atmospheric concentrations in the Arctic.

In the Arctic region, contrary to sulphate aerosols whose burden mainly depends on aerosol transport from polluted areas, the BC burden is driven both by aerosol transport from industrialised areas and by local emissions. Here, 'local emissions' essentially consist of summer biomass burning and are constant from one year to another, as the same inventory is used over the s6 yr of our simulation. The only inter-annual variability we were able to derive in our study, therefore, originates from atmospheric variability. In the real world, biomass burning is highly variable from one year to another (Dentener et al., 2006) and seems to occur increasingly earlier in the season in boreal regions as a result of changing climate (Flannigan et al., 2009). Warneke et al. (2009 and 2010) for instance observed particularly strong carbonaceous aerosol emissions associated with agricultural and forest fires in spring 2008 in Eurasia. Emissions variations should be taken into account to characterise more accurately the inter-annual variation of the Arctic BC load.

4.3. *Mineral dust*

Figure 8 is the same as Figs. 6 and 7 but for mineral dust. The seasonal cycle of the mean mineral dust burden in the Arctic is characterised by two maxima occurring in April and December, with values, respectively, reaching 6 and $4.5\,\mathrm{mg\,m^{-2}}$ (Fig. 8, top left). Minimum values occur in August and January, respectively, reaching 1 and $2\,\mathrm{mg\,m^{-2}}$. Such variations are explained both by the seasonal variations of the emissions and the atmospheric variability. Dust emissions take place far from the Arctic region: Ginoux et al. (2004) estimated that 65% of the global dust emissions take place in North Africa and 25% in Central Asia. These emissions are lower during summer, which explains the low dust burden modelled in the Arctic for this season. The minimums of modelled dust concentrations in the Arctic are also enhanced by the increase in summer precipitation in this region. As local dust emissions are very low in the Arctic, the Arctic dust burden is essentially driven by the transport of dust emitted in the large desert areas of the Northern hemisphere. Dust transport towards the Arctic atmosphere takes mean values of $0.5\,\mathrm{mg\,m^{-2}\,d^{-1}}$ in spring and fall. However, in our simulation, the strongest events of dust transport towards the Arctic region reach weekly mean of $3.5\,\mathrm{mg\,m^{-2}\,d^{-1}}$ (Fig. 8, middle left). The highest emissions of dust over the Earth occur during the northern hemisphere in winter. However, dust transport towards the Arctic is limited in this season: as explained in Sections 4.1. and 4.2, the Arctic region is quite isolated from the atmospheric circulation of temperate regions due to low values of potential temperature. For this reason, the mean dust burden in the Arctic reaches its maximum values in spring and fall. Furthermore, in contrast with global analysis, where dry deposition and sedimentation consist in the main sinks of dust (Textor et al., 2007), wet deposition appears here as the main sinks for dust in the Arctic atmosphere. This is due to the fact that only the smallest particles of mineral dust reach the Arctic atmosphere due to dry deposition and sedimentation affecting coarser particles near the sources. Wet deposition thereby becomes predominant when dust particles are far from their emission region. These small particles have a long residence time (Fig. 8, bottom left), with a noisy seasonal cycle ranging from 9 d in September and October to 15 d in May and June. However, the residence time of mineral dust in the Arctic has strong inter-annual variability: during our 6 yr of simulation, it reached a minimum value of 4 d in October and a maximum value of 30 d at the end of May.

In summer, the dust burden generally does not exceed $1\,\mathrm{mg\,m^{-2}}$ (Fig. 8, top right). See the dust burden distribution in Fig. 8 (top right), both Asian and African emissions seem to impact the Arctic atmosphere during the rest of the year. Alhough weaker than the African source, the Asian source is geographically closer to the North pole. For this reason, it seems to be predominant in the Arctic region. This point has been noticed both in modelling studies (Chin et al., 2007) and in observational campaigns in North of America (Stone et al., 2005; Di Pierro et al., 2011). However, see Fig. 8 (top right), African and middle East sources also seem to impact the Arctic atmosphere, especially in Northern Europe and Russia. In their modelling study, Chin et al. (2007) noticed that particles emitted in these regions could reach the Arctic. In the Canadian Arctic atmosphere, Mc Kendry et al. (2007) observed dust originating from Sahara. Their study suggests that Saharan particles can be transported to very long distances and can, therefore, affect the whole Arctic atmosphere. In spring,

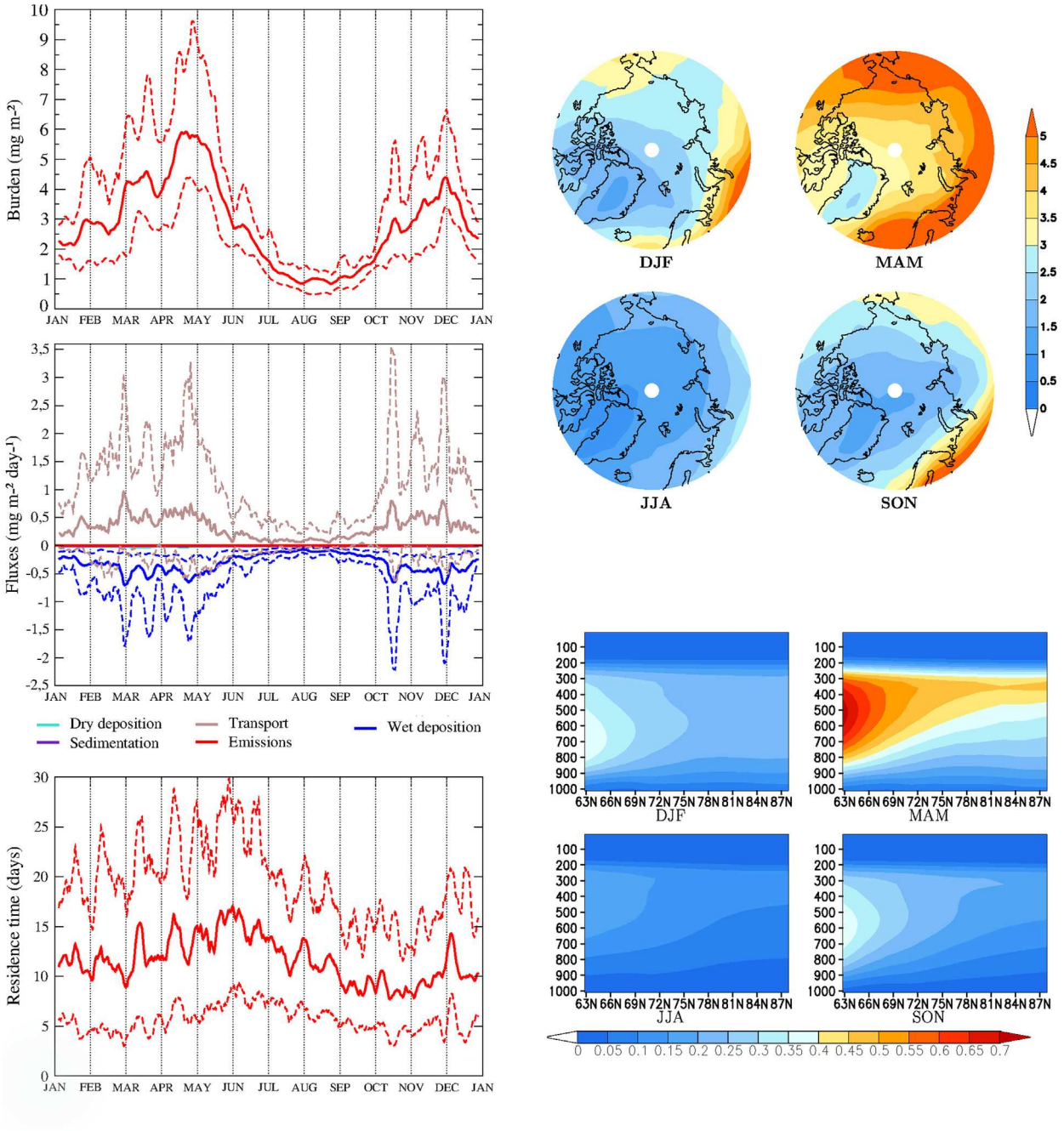

Fig. 8. Left: Burden, sinks, sources and residence time of mineral dust averaged over the Arctic domain. Average is a weekly moving average of the annual cycle over 2000–2005. Dashed lines represent the extreme values reached during the 6-yr simulation. Right, top: dust burden (mg m^{-2}, 2000–2005 seasonal average); right, bottom: zonal mean of dust concentration (μg m^{-3}, 2000–2005 seasonal average, pressure levels in hPa on the vertical axis). All graphs show MOCAGE model outputs.

the dust burden exceeds 5 mg m^{-2} over the whole Northern Eurasia, ranges from 3 to 5 mg m^{-2} over the Arctic Ocean and reaches 3 mg m^{-2} over Greenland, the region of our domain displaying the lowest aerosol concentration. Dust emissions occurring very far from the Arctic region and in regions with high potential temperature, dust aerosols are consequently transported to the Arctic via the upper route (path no. 2 described previously). The maximum of dust atmospheric concentration is, therefore, modelled quite high in the troposphere (Fig. 8, bottom right). In spring,

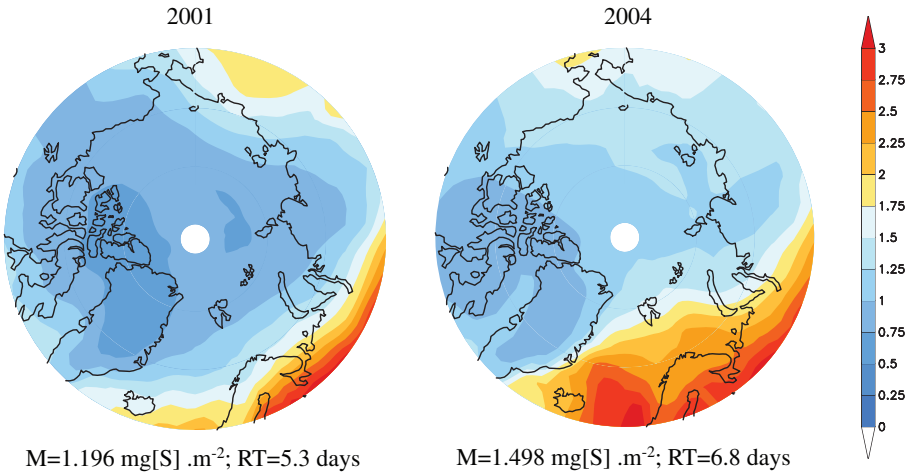

M=1.196 mg[S] .m^{-2}; RT=5.3 days M=1.498 mg[S] .m^{-2}; RT=6.8 days

(a) Sulphate burden (mg[S] .m^{-2})

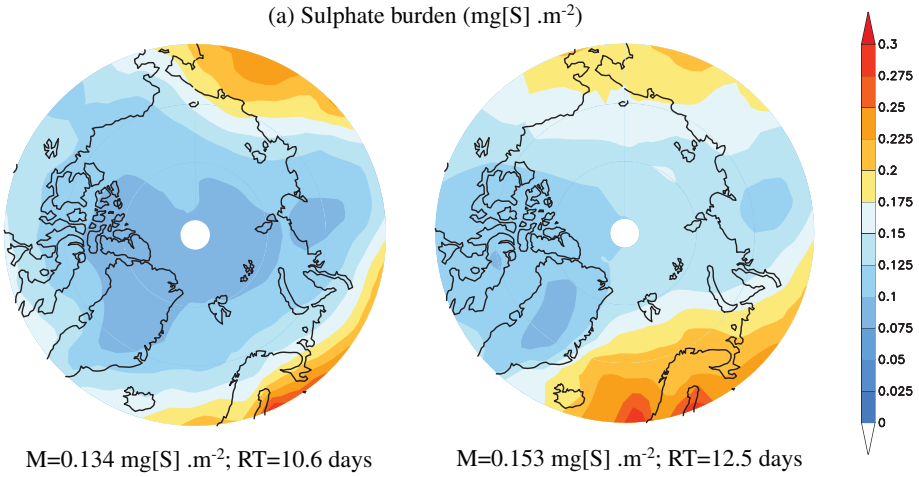

M=0.134 mg[S] .m^{-2}; RT=10.6 days M=0.153 mg[S] .m^{-2}; RT=12.5 days

(b) BC burden (mg[S] .m^{-2})

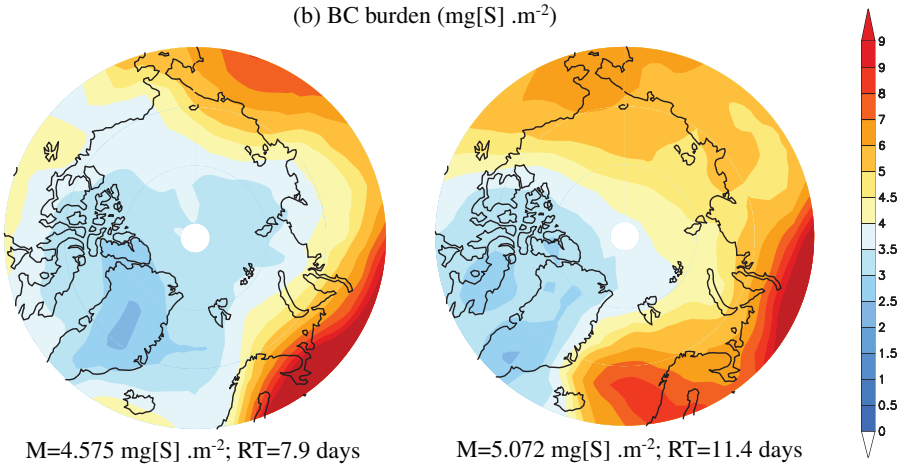

M=4.575 mg[S] .m^{-2}; RT=7.9 days M=5.072 mg[S] .m^{-2}; RT=11.4 days

(c) Mineral dust burden (mg[S] .m^{-2})

Fig. 9. Sulphate, (BC) and mineral dust burden averaged over March–May 2001 (left) and 2004 (right). Mean burden values (M) and Residence Time are indicated under each figure for each aerosol and year.

when the atmospheric load is the highest, maximum zonal means of $0.7\,\mu g\,m^{-3}$ and $0.5\,\mu g\,m^{-3}$ are, respectively, modelled at 500 hPa (i.e. 5 km) at 60 °N and at 350 hPa (i.e. 8 km) at the North Pole. In this season, dust reaches the tropopause. Within the first hundred metres of the atmosphere, the dust zonal mean concentration does not exceed $0.1\,\mu g\,m^{-3}$ all over the year. As high dust concentrations are reached in very high atmospheric layers when compared with sulphate and BC, the high precipitation rates of summer and fall—which essentially involve the low levels of the atmosphere—have less impact on dust wet deposition and residence time. In contrast with sulphate and BC, the burden of dust, therefore, increases also in fall (see Fig. 8, top left and top right).

5. Comparison of the aerosol burden in spring 2001 and spring 2004

As explained in the previous section, the Arctic atmosphere is largely impacted by aerosol transport from lower latitudes in spring. However, this phenomenon is quite variable from one year to another. In particular, the aerosol burden simulated during the springs (MAM) 2001 and 2004 is quite different: Fig. 9 shows the burden of sulphate, BC and mineral dust for these two springs. The seasonal mean burden over the Arctic region in spring 2001 for these three species is respectively equal to $1.196\,mg[S]\,m^{-2}$, $0.134\,mg\,m^{-2}$ and $4.575\,mg\,m^{-2}$. In 2004, these values rose to $1.498\,mg[S]\,m^{-2}$, $0.153\,mg\,m^{-2}$ and $5.072\,mg\,m^{-2}$, which respectively represent increases of 25%, 14% and 10%. Such differences are associated to an increase inthe aerosol residence time: from 5.3 to 6.8 d for sulphate ($\sim$30%), from 10.6 to 12.5 d for BC ($\sim$18%) and from 7.9 to 11.4 d for mineral dust ($\sim$44%).

Higher aerosol burden in spring 2001, when compared to spring 2004, is clearly visible in Northern Europe and Western Russia (Fig. 9). It can be explained by lower precipitation in 2004 in comparison to 2001 over these regions (Fig. 10a). Moreover, the spring 2004 is characterised by a circulation more favourable for aerosol transport from Western Europe compared to spring 2001 (Fig. 10b), accumulating aerosols in the Arctic region. The major part of the mean aerosol burden variability over the whole Arctic region seems to be explained by the variability of the aerosol transport from Europe and Western Russia (Fig. 9). The aerosol burden in the Arctic atmosphere also differs markedly between the springs 2001 and 2004 at two specific places: Northwest of Alaska and north of Eastern Asia. Over Alaska, the aerosol burden (considering the three species sulphate, BC and mineral dust) is slightly higher in spring 2004 than in spring 2001, a difference explained by lower precipitation in spring 2004 over this region. North of Eastern Asia, the aerosol burden is higher in spring 2001 than in spring 2004, which is explained by a higher precipitation rate in 2004 over this region. Overall, the aerosol burden over the Arctic Ocean is largely higher in spring 2004 than in spring 2001, with burden differences reaching 50%.

6. Conclusion

In this paper, we characterised how the atmospheric variability impacts the aerosol burden and residence time in the Arctic region (60 °N to 90 °N). A 6-year global simulation with constant emissions from one year to another was performed to describe the evolution of sulphate, BC and mineral dust. As the aerosol residence time is strongly dependent on wet deposition, an improved representation of this sinks was implemented in our model. Simulations were found to be strongly sensitive to the model representation of the aerosol transfer efficiency towards droplets. Setting a 0.2 lower bound for this parameter—which varies between 0 and 0.9 in our model—reduces the simulated global sulphate burden by 25%. Moreover, considering the aerosol scavenging by ice droplets is crucial as it implies a decrease of 30 to 40% of the global aerosol burden.

The ability of our model to describe the atmospheric concentration of aerosols was inferred by comparisons with results from the models involved in the AEROCOM project (Textor et al., 2006) and from station data: the surface evolution of the sulphate concentration modelled is comparable to observations from North-European stations. At high latitude in Northern America, our model slightly underestimates the sulphate concentration. Concerning BC, the model differs more from observations but simulates a quite realistic annual cycle at the North-European stations. At Northern American stations, there are very large discrepancies between the modelled and the observed BC atmospheric concentrations. Further work is needed in the future to improve the ability of our model to describe aerosols at high latitude. As we found wet deposition to be a key process to describe the aerosol atmospheric concentration, its parameterisation should be improved, thanks to comparisons with observational data, including vertical profiles measured on the course of aircraft campaigns. Still, despite those biases affecting our whole simulation, we assume that we can use our model to analyse how the atmospheric variability affects the aerosol load in the Arctic region. Concerning the atmospheric dust concentration modelled, we did not compare it with observational data, as very few long-term observations are available in the Arctic atmosphere for this aerosol.

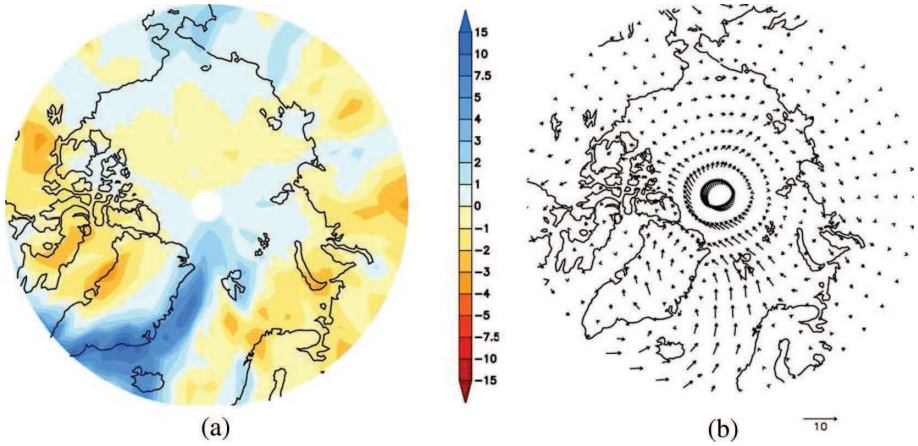

Fig. 10. Precipitation (a, mm d^{-1}) and wind (b, m s^{-1}) differences between MAM 2004 and MAM 2001.

Intra- and inter-annual variations of the burden and the residence time of aerosols were explained, thanks to an analysis of sources and sinks variability. We evaluated the transport of sulphate and BC from polluted area towards northern high latitudes. We also described how the mineral dust emitted in continental deserts can impact the Arctic aerosol burden. The famous 'Arctic haze' occurring in spring is characterised, with weekly averaged sulphate, BC and dust burden reaching, respectively, 1.9 mg[S] m^{-2}, 0.2 mg m^{-2} and 6 mg m^{-2} in the Arctic region. The choice of constant emissions over our 6-year simulation allows evaluating the inter-annual variation of the Arctic aerosol load induced by atmospheric variability. From one year to another, the spring maximum burden averaged over the whole Arctic region can vary within a 20% range for sulphate, a 10% range for BC and a 60% range for mineral dust. Such variations are explained both by transport and wet deposition variabilities. In this study, both processes were characterised by aerosol residence times. Over our 6-year simulation, the weekly means of the aerosols residence times display a strong annual cycle. It takes minimum values in fall or in winter: 4 d for sulphate and 8 d for BC and dust. Maximum values occur in June: 10 d for sulphate and 16 d for BC and dust. However, these extremums can vary by about 50% for sulphate, 40% for BC and 100% for dust from one year to another, in relation to the inter-annual variability of the aerosol burden. In particular, the seasonal mean of the atmospheric burden of sulphate, BC and dust increases, respectively, by 25%, 14% and 10% between the spring 2001 and 2004. These variations are induced by different wind and precipitation conditions. They are associated to an increase in the residence time of 30% for sulphate, 18% for BC and 44% for dust.

As the estimation of aerosol residence time through observations is still quite uncertain (e.g. Baskaran and Shaw, 2001), models appear as a useful tool to evaluate it and characterise *in fine* the equilibrium between aerosols sinks and sources. However, future developments should focus on improving the parameterisation of aerosols sinks in the models. In particular, wet deposition should depend on cloud characteristics to be more realistic and to improve, therefore, the evaluation of the aerosol residence time in the Arctic.

7. Acknowledgements

We thank all the groups who provided us the aerosol data used in this study: Anne-G. Hjellbrekke and the EMEP program (European data); the U.S. National Park Service (Denali data downloaded from the IMPORT website); the Climate Change Measurement Research (CCMR) from the Climate Research Division (CRD), Environment Canada (Alert data); the NOAA/ESRL/GMD and DOE's ARM Program (Barrow data). In particular, we thank P.K. Quinn for helping us to analyse sulphate data from Barrow. This work was funded by Météo-France, CNRS and by the projects 'Agence Nationale pour la Recherche NEEM' and 'European Commission LIFE FP7 SNOW-CARBO'. The figures have been prepared with GRADS and SCILAB free software. We are grateful to the two anonymous referees for their comments that helped to improve this article.

References

Baskaran, M. and Shaw, G. E. 2001. Residence time of Arctic haze aerosols using the concentrations and activity ratios of 210Po, 210Pb, and 7Be. *J. Aerosol Sci.* **32**(4), 17–26.

Bechtold, P., Bazile, E., Guichard, F., Mascart, P. and Richard, E. 2001. A mass flux convection scheme for regional and global models. *Q. J. Roy. Meteor. Soc.* **127**, 869–886.

Boucher, O., Pham, M. and Venkataraman, C. 2002. Simulation of the atmospheric sulfur cycle in the Laboratoire de Météorologie Dynamique General Circulation Model. Model Description, Model Evaluation, and Global and European Budgets, Note no. **23**, IPSL. http://icmc.ipsl.fr/outcomes/reports-a-notes/icmc-scientific-notes.

Bourgeois, Q. and Bey, I. 2011. Pollution transport efficiency toward the Arctic: sensitivity to aerosol scavenging and source regions. *J. Geophys. Res.* **116**, D08213, doi:10.1029/2010JD015096.

Cavalli, F., Viana, M., Yttri, K. E., Genberg, J. and Putaud, J.-P. 2010. Toward a standardised thermal-optical protocol for measuring atmospheric organic and elemental carbon: the EUSAAR protocol. *Atmos. Meas. Tech.* **3**, 79–89.

Chin, M., Diehl, T., Ginoux, P. and Malm, W. 2007. Intercontinental transport of pollution and dust aerosols: implications for regional air quality. *Atmos. Chem. Phys.* **7**, 5501–5517, doi:10.5194/acp-7-5501-2007.

Conant, W. C., Nenes, A. and Seinfeld, J. H. 2002. Black carbon radiative heating effects on cloud microphysics and implications for aerosol indirect forcing, 1, Extended Köhler theory. *J. Geophys. Res.* **107**(D21), 4604, doi:10.1029/2002JD002094.

Cozic, J., Verheggen, B., Mertes, S., Connolly, P., Bower, K. and co-authors. 2007. Scavenging of black carbon in mixed phase clouds at the high alpine site Jungfraujoch. *Atmos. Chem. Phys.* **7**, 1797–1807, doi:10.5194/acp-7-1797-2007.

de Meij, A., Krol, M., Dentener, F., Vignati, E., Cuvelier, C. and co-authors. 2006. The sensitivity of aerosol in Europe to two different emission inventories and temporal distribution of emissions. *Atmos. Chem. Phys.* **6**, 4287–4309, doi:10.5194/acp-6-4287-2006.

Dentener, F., Kinne, S., Bond, T., Boucher, O., Cofala, J. and co-authors. 2006. Emissions of primary aerosol and precursor gases in the years 2000 and 1750 prescribed data-sets for AeroCom. *Atmos. Chem. Phys.* **6**, 4321–4344.

Di Pierro, M., Jaeglé, L. and Anderson, T. L. 2011. Satellite observations of aerosol transport from East Asia to the Arctic: three case studies. *Atmos. Chem. Phys.*, **11**, 2225–2243, doi:10.5194/acp-11-2225-2011.

Flanner, M. G., Zender, C. S., Randerson, J. T. and Rasch, P. J. 2007. Present-day climate forcing and response from black carbon in snow. *J. Geophys. Res.* **112**, D11202, doi:10.1029/2006JD008003.

Flannigan, M. D., Stocks, B. J., Turetsky, M. R. and Wotton, B. M. 2009. Impact of climate change on fire activity and fire management in the circumboreal forest. *Global Change Biology*, **15**, 549–560. doi: 10.1111/j.1365-2486.2008.01660.x.

Ginoux, P., Prospero, J. M., Torres, O. and Chin, M. 2004. Long-term simulation of global dust distribution with the GOCART model: correlation with North Atlantic Oscillation. *Environ Model. Software* **19**, 113–128.

Gong, S. L., Zhao, T. L., Sharma, S., Toom-Sauntry, D., Lavoué, D. and co-authors. 2010. Identification of trends and interannual variability of sulfate and black carbon in the Canadian High Arctic: 1981–2007. *J. Geophys. Res.*, **115**, D07305, doi:10.1029/2009JD012943.

Greenaway, K. R. 1950. Experiences with Arctic flying weather. Report, *Royal Meteorol. Soc. Can. Branch*. Toronto, Ont., Canada.

Henning, S., Bojinski, S., Diehl, K., Ghan, S., Nyeki, S. and co-authors. 2004. Aerosol partitioning in natural mixed-phase clouds, *Geophys. Res. Lett.* **31**, L06101, doi:10.1029/2003GL019025.

Hirdman, D., Burkhart, J. F., Sodemann, H., Eckhardt, S., Jefferson, A. and co-authors. 2010. Long-term trends of black carbon and sulphate aerosol in the Arctic: changes in atmospheric transport and source region emissions. *Atmos. Chem. Phys.* **10**, 9351–9368, doi:10.5194/acp-10-9351-2010.

Hitzenberger, R., Berner, A., Glebl, H., Drobesch, K., Kasper-Giebl, A. and co-authors. 2001. Black carbon (BC) in alpine aerosols and cloud water-concentrations and scavenging efficiencies. *Atmos. Env.* **35**, 5135–5141, doi:10.1016/S1352-2310(01)00312-0.

Hjellbrekke, A.-G. 2004. Data report 2002, acidifying and eutrophying compounds, *Tech. Rep.* EMEP/CCC Rep. 1/2004, EMEP, Oslo, Norway.

Intergovernmental Panel on Climate Change (IPCC). 2007. *Climate Change 2007: The Physical Science Basis. Contribution of Working Group I to the Fourth Assessment Report of the Intergovernmental Panel on Climate Change* (S. Solomon et al. eds.) Cambridge University Press, Cambridge, U K., 996 pp.

Jacobson, M. Z. 2004. Climate response of fossil fuel and biofuel soot, accounting for soot's feedback to snow and sea ice albedo and emissivity. *J. Geophys. Res.* **109**, D21201, doi:10.1029/2004JD004945.

Josse, B., Simon, P. and Peuch, V.-H. 2004. Rn-222 global simulations with the multiscale CTM MOCAGE. *Tellus* **56B**, 339–356.

Kasper-Gibel, A., Koch, A., Hitzenberger, R. and Puxbaum, H. 2000. Scavenging Efficiency of 'Aerosol Carbon' and Sulfate in Supercooled Clouds at Mt. Sonnblick (3106 m a.s.l., Austria). *J. Atmos. Chem.* **35**, 33–46.

Klonecki, A., Hess, P., Emmons, L., Smith, L., Orlando, J. and co-authors. 2003. Seasonal changes in the transport of pollutants into the Arctic troposphere—Model study. *J. Geophys. Res.*, **108**(D4), 8367, doi:10.1029/2002JD002199.

Koch, D., Schulz, M., Kinne, S., McNaughton, C., Spackman, J. R. and co-authors. 2009. Evaluation of black carbon estimations in global aerosol models. *Atmos. Chem. Phys.* **9**, 9001–9026, doi:10.5194/acp-9-9001-2009.

Lamarque, J.-F., Bond, T. C., Eyring, V., Granier, C., Heil, A. and co-authors. 2010. Historical (1850–2000) gridded anthropogenic and biomass burning emissions of reactive gases and aerosols: methodology and application. *Atmos. Chem. Phys.* **10**, 7017–7039, doi:10.5194/acp-10-7017-2010.

Langner, J. and Rodhe, H. 1991. A global three-dimensional model of the tropospheric sulphur cycle. *J. Atmos. Chem.* **13**, 225–263.

Lavoué, D., Liousse, C., Cachier, H., Stocks, B. J. and Goldammer, J. G. 2000. Modeling of carbonaceous particles emitted by boreal and temperate wild-fires at northern latitudes. *J. Geophys. Res.* **105**, 26 890.

Louis, J.-F. 1979. A parametric model of vertical eddy-fluxes in the atmosphere. Bound. Lay. *Meteor.* **17**, 187–202.

Mari, C., Jacob, D. J. and Betchold, P. 2000. Transport and scavenging of soluble gases in a deep convective cloud. *J. Geophys. Res.* **105,** D17, 22 255.

Martet, M., Peuch, V.-H., Laurent, B., Marticorena, B. and Marticorena, G. 2009. Evaluation of long-range transport and deposition of desert dust with the CTM MOCAGE. *Tellus* **61B**, 449–463.

McKendry, I. G., Stawbridge, K. B., O'Neill, N. T., Macdonald, A. M., Liu, P. S. K. and co-authors. 2007. Trans-Pacific transport of Saharan dust to western North America: A case study, *J. Geophys. Res.* **112**, D01103, doi:10.1029/2006JD007129.

Ménégoz, M., Salas y Melia, D., Legrand, M., Teyssèdre, H., Michou, M. and co-authors. 2009. Equilibrium of sinks and sources of sulphate over Europe: comparison between a six-year simulation and EMEP observations. *Atmos. Chem. Phys.* **9**, 4505–4519, doi:10.5194/acp-9-4505-2009.

Michou, M. and Peuch, V.-H. 2002. Surface exchanges in the MOCAGE multiscale Chemistry and Transport Model. *J. Water Sci.* **15**, 173–203.

Nho-Kim, E.-Y., Michou, M. and Peuch, V.-H. 2004. Parameterization of size dependent particle dry deposition velocities for global modelling. *Atmos. Environ.* **38**, 1933–1942.

Pacyna, J. M., Ottar, B., Tamza, U. and Maenhaut, W. 1986. Long-range transport of trace elements to Ny Alesund, Spitsbergen. *Atmos. Envir.* **19**, 857–865.

Penner, J. E., Andreae, M., Annegarn, H., Barrie, L., Feichter, J. and co-authors. 2001. Aerosols, their Direct and Indirect Effects, in: *Climate Change 2001: The Scientific Basis* (Houghton, J. T., Ding, Y., Griggs, D. J., Noguer, M. Van der Linden, P. J., Dai, X., Maskell, K. and Johnson, C. A. eds.), *Report to Intergovernmental Panel on Climate Change from the Scientific Assessment Working Group (WGI)*, Cambridge University Press, 289–416.

Pham, M., Müller, J.-F., Brasseur, G. P., Granier, C. and Mégie, G. 1995. A three-dimensionnal study of the tropospheric sulphur cycle. *J. Geophys. Res.* **100**, 26061–26092.

Prank, M., Sofiev, M., Denier van der Gon, H. A. C., Kaasik, M., Ruuskanen, T. M. and co-authors. 2010. A refinement of the emission data for Kola Peninsula based on inverse dispersion modeling. *Atmos. Chem. Phys.* **10**, 10849–10865, doi:10.5194/acp-10-10849-2010.

Quinn, P. K., Bates, T. S., Miller, T. L., Coffman, D. J., Johnson, J. E. and co-authors. 2000. Surface submicron aerosol chemical composition: What fraction is not sulfate? *J. Geophys. Res.* **105**(D5), 6785–6805.

Reddy, M. S., Boucher, O., Bellouin, N., Schulz, M., Balkanski, Y. and co-authors. 2005. Estimates of global multicomponent aerosol optical depth and direct radiative perturbation in the Laboratoire de Météorologie Dynamique general circulation model. *J. Geophys. Res.* **110**, D10S16, doi:10.1029/2004JD004757.

Riemer, N., Vogel, H. and Vogel, B. 2004. Soot aging time scales in polluted regions during day and night, *Atmos. Chem. Phys.* **4**, 1885–1893, doi:10.5194/acp-4-1885-2004.

Scheuer, E., Talbot, R. W., Dibb, J. E., Seid, G. K., DeBell, L. and co-authors. 2003. Seasonal distributions of fine aerosol sulfate in the North American Arctic basin during TOPSE. *J. Geophys. Res.* **108**(D4), 8370, doi:10.1029/2001JD001364.

Seinfeld, J. H. and Pandis, S. N. 2006. *Atmospheric Chemistry and Physics: From Air Pollution to Climate Change* (second edition, John Wiley). New York. 1203 pp.

Sharma, S., Andrews, E., Barrie, L. A., Ogren, J. A. and Lavoué, D. 2006. Variations and sources of the equivalent black carbon in the high Arctic revealed by long-term observations at Alert and Barrow: 1989–2003. *J. Geophys. Res.* **111**, D14208, doi:10.1029/2005JD006581.

Sharma, S., Lavoué, D., Cachier, H., Barrie, L. A. and Gong, S. L. 2004. Long-term trends of the black carbon concentrations in the Canadian Arctic. *J. Geophys. Res.* **109**, D15203, doi:10.1029/2003JD004331.

Shaw, G. E. 1995. The Arctic Haze phenomenon. *Bull. Am. Meteorol. Soc.* **76**, 2403–2412.

Shindell, D. T., Chin, M., Dentener, F., Doherty, R. M., Faluvegi, G. and co-authors. 2008. A multi-model assessment of pollution transport to the Arctic. *Atmos. Chem. Phys.* **8**, 5353–5372, doi:10.5194/acp-8-5353-2008.

Stier, P., Feichter, J., Kinne, S., Kloster, S., Vignati, E. and co-authors. 2005. The aerosol-climate model ECHAM5-HAM. *Atmos. Chem. Phys.* **5**, 1125–1156, doi:10.5194/acp-5-1125-2005.

Stohl, A. 2006. Characteristics of atmospheric transport into the Arctic troposphere. *J. Geophys. Res.* **111**, D11306, doi:10.1029/2005JD006888.

Stone, R., Anderson, G., Andrews, E., Dutton, E., Harris, J. and co-authors. 2005. Asian dust signatures at Barrow: observed and simulated. Incursions and impact of Asian dust over Northern Alaska. *Workshop on Remote Sensing of Atmospheric Aerosols, IEEE Conference Proceedings*, doi:10.1109/AERSOL.2005.1494152, 74–79.

Textor, C., Schulz, M., Guibert, S., Kinne, S., Balkanski, Y. and co-authors. 2006. Analysis and quantification of the diversities of aerosol life cycles within AeroCom. *Atmos. Chem. Phys.* **6**, 1777–1813.

Textor, C., Schulz, M., Guibert, S., Kinne, S., Balkanski, Y. and co-authors. 2007. The effect of harmonized emissions on aerosol properties in global models – an AeroCom experiment. *Atmos. Chem. Phys.* **7**, 4489–4501, doi:10.5194/acp-7-4489-2007.

Teyssèdre, H., Michou, M., Clark, H. L., Josse, B., Karcher, F. and co-authors. 2007. A new tropospheric and stratospheric Chemistry and Transport Model MOCAGE-Climat for multi-year studies: evaluation of the present-day climatology and sensitivity to surface processes. *Atmos. Chem. Phys.* **7**, 5815–5860.

Vignati, E., Karl, M., Krol, M., Wilson, J., Stier, P. and co-authors. 2010. Sources of uncertainties in modelling black carbon at the global scale, *Atmos. Chem. Phys.* **10**, 2595–2611, doi:10.5194/acp-10-2595-2010.

Warneke, C., Bahreini, R., Brioude, J., Brock, C. A., de Gouw, J. A. and co-authors. 2009. Biomass burning in Siberia and Kazakhstan as an important source for haze over the Alaskan

Arctic in April 2008. *Geophys. Res. Lett.* **36**, L02813, doi:10.1029/2008GL036194.

Warneke, C., Froyd, K. D., Brioude, J., Bahreini, R., Brock, C. A. and co-authors. 2010. An important contribution to springtime Arctic aerosol from biomass burning in Russia. *Geophys. Res. Lett.* **37**, L01801, doi:10.1029/2009GL041816.

Wesely, M. L. 1989. Parameterization of surface resistances to gaseous dry deposition in regional-scale numerical models. *Atmos. Environ.* **23**, 1293–1304.

Williamson, D. L. and Rash, P. J. 1989. Two-dimensional semilagrangian transport with shape-preserving interpolation. *Mon. Weather Rev.* **117**, 102–129.